Magnetic Nanoparticle Dynamics and Assembly Phenomena in External Magnetic Fields

Xiaozheng Xue[1] and Edward P. Furlani[1, 2]

[1] Dept. of Chemical and Biological Engineering, University at Buffalo SUNY,
Email:xiaozhen@buffalo.edu

[2]Dept. of Electrical Engineering,
University at Buffalo SUNY, Office: (716) 645-1194 Fax: (716) 645-3822, Email:efurlani@buffalo.edu

ABSTRACT

A computational model is introduced for predicting the field-directed assembly of colloidal magnetic particles under the influence of a high-gradient magnetic field and the manipulation of assembled particle microstructures in a time-varying field. The model is based on a modified discrete element method and takes into account several competitive effects including the applied-magnetic force, induced magnetic dipole-dipole interactions, Brownian dynamics, Van der Waals interaction, viscous drag and hydrodynamic interactions among the particles. A dynamic time-stepping approach introduced to stabilize and accelerate the computation. The model is useful for predicting the formation of self-assembled micro and nano structures of magnetic nanoparticles and the stability of such structures in a time-varying field. The model is demonstrated via application to various nanoparticle systems.

Keywords: magnetic nanoparticle self-assembly, magnetic dipole-dipole interactions, magnetic particle chains, magnetic particle chain dynamics in a time-varying magnetic field.

1 INTRODUCTION

The interest in magnetic particles and ferrofluids has grown substantially in recent years as their applications continue to proliferate. Current applications include field-directed transport of biomolecules and therapeutic drugs [1], enhanced gene transfection [2,3], bioseparation and sorting [4], high-density magnetic data storage, ferrofluid seals and pumps, microfluidic mixers, and highly sensitive magnetoresistive-based sensors, among many others. However, despite the widespread and growing use of magnetic nanoparticles, there are many fundamental aspects of their collective behavior that remain unknown. Areas of particular interest are use of field-directed assembly to form micro and nanostructured magnetic media and the controlled manipulation of assembled structures using time-varying fields. In this paper, we present a computational model for predicting the assembly of magnetic particles using high-gradient fields and the dynamics of particle-based microstructures in time-dependent fields. The model involves the numerical integration of a Langevin equation that accounts for interparticle dipole-dipole effects, (that drive particle assembly), viscous drag, fluid-mediated (hydrodynamic) particle-particle interactions and Smoluchowski's theory of Brownian motion. We use dynamic time-stepping and analytical expressions for the magnetic force to greatly accelerate and stabilize the computations. We discuss the model in detail and demonstrate its use in the analysis of both high-gradient and time-varying magnetic particle systems (Fig. 1).

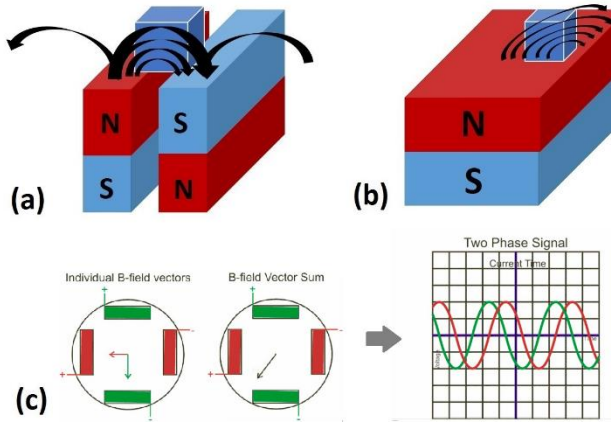

Fig.1 Magnetic particle systems and fields: (a),(b) computational domain and field gradient in (a) the gap region between two rare-earth magnets; and (b) at the edge of a single magnet; and (c) time-harmonic magnetic field components for investigating the stability of magnetic particle microstructures

2 THEORY AND MODELING

The behavior of colloidal magnetic particles under the influence of an applied field is governed by several factors. These include the applied magnetic force, interparticle dipole-dipole interactions, fluidic drag, Van der Waals

force, Brownian dynamics and interparticle hydrodynamic interactions due to lubrication effects. We include these effects into our model as force terms in a Langevin equation. We predict the assembly of magnetic particles and the motion of particle microstructures by numerically integrating this equation using a self-adjusted time step to accelerate and stabilize the computation. The various terms in the model and its implementation are described in detail in the following sections.

2.1 Magnetic Force

The magnetic force on a magnetic particle is computed using the "effective" dipole moment method in which the particle is modeled as an "equivalent" point dipole with an effective moment $\boldsymbol{m}_{eff}$. The force on the particle is given by

$$F_{m,i} = \mu_f (m_{i,eff} \cdot \nabla) H_a \tag{1}$$

where μ_f is the permeability of the fluid and $\boldsymbol{H}_a$ is the applied magnetic field intensity at the center of particle. The moment $\boldsymbol{m}_{eff}$ can be determined using a magnetization model that takes into account self-demagnetization and magnetic saturation of the particles [1]

$$\boldsymbol{m}_{i,eff} = V_p f(H_a) \boldsymbol{H}_a \tag{2}$$

where

$$f(H_a) = \begin{cases} \dfrac{3(\chi_p - \chi_f)}{(\chi_p - \chi_f) + 3} & H_a < \left(\dfrac{(\chi_p - \chi_f) + 3}{3\chi_p}\right) M_{sp} \\ M_{sp}/H_a & H_a \geq \left(\dfrac{(\chi_p - \chi_f) + 3}{3\chi_p}\right) M_{sp} \end{cases} \tag{3}$$

Here, $V_p = \frac{4}{3}\pi R_p^3$ is the volume of particle, χ_p and χ_f are the magnetic susceptibilities of the particle and fluid, respectively, M_{sp} is the saturation magnetization of the particle. Thus, the magnetic force can be rewritten as

$$\boldsymbol{F}_{m,i} = \mu_f V_p f(H_a)(\boldsymbol{H}_a \cdot \boldsymbol{\nabla}) \boldsymbol{H}_a. \tag{4}$$

This can be determined once an expression for the applied field is known. The field can be obtained in closed-form for isolated rare-earth permanent magnet structures.

2.2 Magnetic Dipole-Dipole Interactions

In the presence of an applied magnetic field, superparamagnetic nanoparticles become magnetized and aquire a magnetic moment $\boldsymbol{m}_{eff}$ as described above. The dipole-dipole potential energy between particles is given by the following equation

$$H_{dd,ij} = -\frac{\mu_f}{4\pi}\left(3\frac{(\boldsymbol{m}_{i,eff}\cdot\boldsymbol{r}_{ij})(\boldsymbol{m}_{j,eff}\cdot\boldsymbol{r}_{ij})}{r_{ij}^5} - \frac{\boldsymbol{m}_{i,eff}\cdot\boldsymbol{m}_{j,eff}}{r_{ij}^3}\right) \tag{5}$$

where $\boldsymbol{m}_{i,eff}$ and $\boldsymbol{m}_{j,eff}$ are the effective magnetic moments of particles i and j, respectively, $\boldsymbol{r}_{ij}$ is the displacement vector between two particles. The magnetic dipole-dipole force is obtained as the gradient of the potential,

$$\boldsymbol{F}_{dd,ij} = -\boldsymbol{\nabla} H_{dd,ij}. \tag{6}$$

2.3 Van der Waals interaction

The Van der Waals force is taken into account in two parts, i.e. attractive and repulsive force components. We assume that the nanoparticles are hard spheres, which means that they cannot compress each other. The repulsive force is used to prohibit particle overlap.

The attractive part of Van der Waals interaction is calculated using the following expression:

$$\boldsymbol{F}_{vdw,ij} = \frac{A}{6}\frac{d_i^6}{(h_{ij}^2 + 2d_i h_{ij})^2 (h_{ij} + d_i)^3} \tag{7}$$

where A is the Hamaker constant and h_{ij} is the surface-to-surface separation distance between particles i and j. At any time step, if the surface-to-surface distance is less than 1% of particle diameter, h_{ij} is reset to 1% of the radius to avoid particle overlapping.

Based on the potential model proposed by Buckinghan, the repulsive part of Van der Waals interaction is exponential, i.e.

$$\boldsymbol{F}_{rep,ij} = K_1 e^{K_2\left(\frac{r_{ij}}{2R_p} - 1\right)} \tag{8}$$

where K_1 and K_2 are parameters depending on the material of nanoparticle and fluid properties. Here, we assume that $K_1 = \frac{3\mu_f(\boldsymbol{m}_{i,eff}\cdot\boldsymbol{m}_{j,eff})}{32\pi R_p^4}$ in order to balance the magnetic dipole-dipole force to avoid partice overlapping. K_2 is a constant and must be negative to give a decaying characteristic. It is selected via a trial and error approach. On one hand, a large K_2 gives rise to a steeper decay, which more closely approximates reality. However, a large number will make the repulsive force extremely large for small distances, which leads to numerical instability. A value of $K_2 = -50$ was chosen as a balance between these two competing factors based on numerical experiments.

2.4 Hydrodynamic Interaction Effects

Hydrodynamic interactions between particles become important at small surface-to-surface separation distances. The force between two neighboring particles is based on lubrication theory and can be expressed as follows

$$\boldsymbol{F}_{lub,ij} = \frac{6\pi\mu_f \boldsymbol{V}_r}{h_{ij}}\frac{d_i^2}{16} \tag{9}$$

This force depends on the surface-to-surface separation distance h_{ij} and the relative velocity $\boldsymbol{V}_r$ between neighboring particles. Also, in this model, when the surface-to-surface distance is less than 1% of particle radius, h_{ij} is reset tot 1% of the radius to avoid the particle overlap.

2.5 Brownian Motion

Brownian motion must be considerd when predicting the dynamics of nanoscale particles. We use the following equation to account fro these effects

$$< x^2 >= \frac{RT}{6\pi\eta R_p N} \cdot (2\Delta t) = \frac{2k_B T}{D} \cdot \Delta \mathrm{t} \qquad (10)$$

where k_B is Boltzmann's constant and $D = 6\pi\eta R_p$ is the Stokes' drag coefficient.

2.6 Netwon's Equation of Motion

Particle motion is predicted using Newton's law of motion:

$$m_i \frac{d^2 \boldsymbol{x}_i}{dt^2} = \boldsymbol{F}_{to;,i} + \boldsymbol{F}_{D,i} \qquad (11)$$

$$\boldsymbol{F}_{to;,i} = \boldsymbol{F}_{m,i} + \sum_{\substack{j=1 \\ j \neq i}}^{N} \left(\boldsymbol{F}_{dd,ij} + \boldsymbol{F}_{vdw,ij} + \boldsymbol{F}_{rep,ij} + \boldsymbol{F}_{lub,ij}\right)$$

where $\boldsymbol{x}_i(t)$ is the trajectory of the i'th particle and $\boldsymbol{F}_D$ is the viscous drag force

$$\boldsymbol{F}_{D,i} = D \frac{d\boldsymbol{x}_i}{dt}. \qquad (12)$$

In this equation $D = 6\pi\eta R_p$ is the Stokes' drag coefficient, k_B is the Boltzmann constant, and η is the fluid viscosity. After combining Eqs. (11) and (12) we obtain

$$m_i \frac{d^2 \boldsymbol{x}_i}{dt^2} + D \frac{d\boldsymbol{x}_i}{dt} = \boldsymbol{F}_{to;,i} \qquad (13)$$

The left-hand side of Eq. (13) represents the trajectory of a an individual particle, while the right-hand side represents the total force acting on it. This second order equation can be reduced to a system of first order equations, which cane be numerically integrated ato achieve equation (14) and (15), which includes a time step τ:

$$\Delta \boldsymbol{x}_i = \frac{\boldsymbol{F}_{tol,i}}{D}\tau + \frac{m_i}{D}\left(\boldsymbol{v}_{i,0} - \frac{\boldsymbol{F}_{tol,i}}{D}\right)\left(1 - e^{-\frac{D}{m_i}\tau}\right) \qquad (14)$$

$$\boldsymbol{v}_{i,f} = \frac{\boldsymbol{F}_{tol,i}}{D} + \left(\boldsymbol{v}_{i,0} - \frac{\boldsymbol{F}_{tol,i}}{D}\right) e^{-\frac{D}{m_i}\tau} \qquad (15)$$

where τ is a time step and $\boldsymbol{v}_{i,0}$ and $\boldsymbol{v}_{i,f}$ are the velocity of particle at the beginning and ending of this time step, and $\Delta \boldsymbol{x}_{B,i}$ is the displacement due to the Brownian motion. Here, the time step τ is designed as a self-adjusted time step, which is determined by the relative velocities $\boldsymbol{V}_r$ and surface-to-surface separation distance h_{ij} to accelerate the simulation process. When the time step τ is large enough ($\tau \gg \frac{m_i}{D}$) and Brownnian motion is taken into consideration, Eq. (14) and (15) can be simplified as follows

$$\Delta \boldsymbol{x}_i = \frac{\boldsymbol{F}_{tol,i}}{D}\tau + \frac{m_i}{D}\left(\boldsymbol{v}_{i,0} - \frac{\boldsymbol{F}_{tol,i}}{D}\right) + \Delta \boldsymbol{x}_{B,i}. \qquad (16)$$

$$\boldsymbol{v}_{i,f} = \frac{\boldsymbol{F}_{tol,i}}{D} \qquad (17)$$

In the folowing anaysis τ is self-adjusted (usually, $10^2 \frac{m_i}{D} < \tau < \frac{h_{ij}}{3V_{r,ij}}$) to accelerate the simulation.

3 RESULTS

We demonstrate the model by predicting particle dynamics and self-assembly in high-gradient fields as shown in Fig. 1a,b and rotation of an assembled chain of particles in a sinusoidally time-varying field as shown in Fig.1c. Fig.2 and Fig 3 show the simulation results achieved from our model. The particles are assumed to be Fe_3O_4, which has a density of $\rho_p = 5{,}000\ kg/m^3$ and saturation magnetization $M_{sp} = 4.78 \times 10^5\ A/m$.

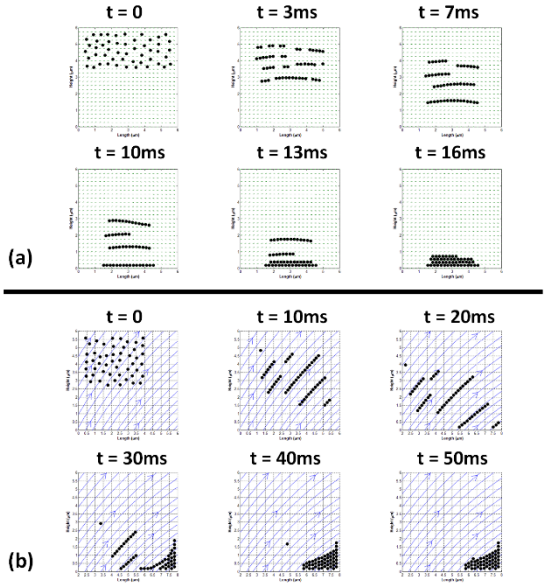

Figure 2. Dynamics and assembly of magnetic nanoparticles in gradient magnetic fields: the computational domain is located (a) the in the gap between two rare-earth magnets as shown in Fig. 1a; (b) at the edge of one isolated magnet as shown in Fig. 1b.

Figure 2a shows a time sequence of the dynamics of magnetic particles ($R_p = 100\ mm$) in water in the gradient

field shown in Fig. 1a. The field is provided by two infinite rectangular rare-earth magnets with a height and width of 100 μm and 40 μm respectively. The magnetization of the magnets is $M_s = 9.55 \times 10^5\ A/m$ and there is a 4μm gap between them. The particles are initially at rest and randomly distributed in the computational domain, which has impermeable walls. The model predicts that the particles assemble into a close packed film above the gap within 16 ms. A similar analysis is shown in Fig.2b, where the computational domain is now located at the edge of a single isolated rectangular magnet as shown in Fig. 1b. The magnet has a height and width of 100 μm and 60 μm, respectively. It takes approximately 50 ms for the particles to form a close packed structure at the edge of the magnet where the field gradient is highest. These simulations took approximately 12 hours to complete on a workstation. In both simulations, we find that the particles do not move in isolation, but rather tend to assemble with neighboring particles during the transport process.

Next we study the stability of particle chains in a rotating field with components as shown in Fig. 1c. We investigate the stability of this microstructure as function of its length and the rotation frequency of the fields. As shown in Fig. 3, different chain lengths respond differently. For a short 9 particle chain in a low 100 Hz frequency field, the chain is stable and responds to the field rotation without delay (Fig. 3a). There is a slight delay when the chain is

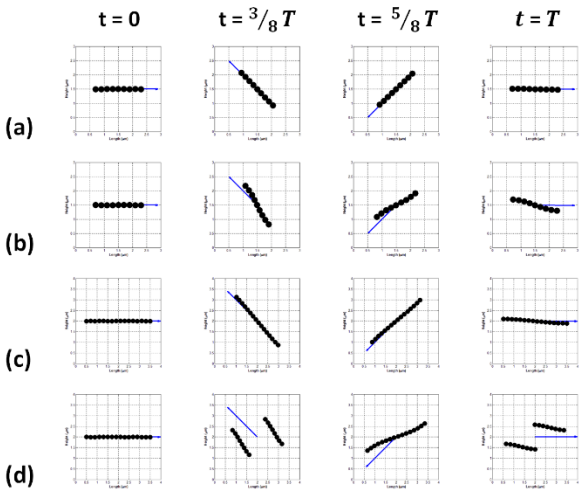

Fig.3 Microstructure of particles' chains in time-varying magnetic field with different frequency: (a) a 9-partile chain in a 100 Hz field; (b) a 9-partile chain in a 1000 Hz field; (c) a 16-partile chain in a 100 Hz field; (d) a 16-partile chain in a 1000 Hz field.

subjected to a 1000 Hz field (Fig. 3b). On the other hand, a longer 16 particle chain exhibits a delay with respect to the field even at 100 Hz (Fig. 3c). The reason for this is because the viscous drag increases with chain length. At a higher frequency of 1000Hz the longer chain becomes unstable and breaks into two smaller chains at its center as shown in Fig. 3d [5,6]. These separate chains rotate independently with the external field without delay. They temporarily reassemble into a longer chain and then break apart again in a time-wise periodic fashion. This behavior, and the ability to predict it, could be useful for applications in microrheology and micromixing.

4 CONCLUSIONS

We have presented a computational model for predicting the dynamics and assembly of magnetic particles in gradient and time-varying magnetic fields. We have used the model to study the assembly process and have found that interparticle dipole-dipole interactions are more important for smaller particle ($R_p < 10^2 nm$) systems. We have investigated the behavior of chain-like particle microstructures in rotating magnetic fields and found that their stability depends on their length (i.e. number of particles) and the frequency of the field rotation. The stability decreases with increasing frequency because of the effects of higher viscous drag. The model presented here is relatively easy to implement and runs efficiently on a stand-alone workstation. It should be of considerable use in the development of a broad range of novel materials and processes involving magnetic nanoparticles and ferrofluids.

REFERENCES

[1] E. P. Furlani, Magnetic Biotransport: Analysis and Applications, Materials, 3(4): 2412-2446, 2010.

[2] E. P. Furlani and X. Xue, Field, force and transport analysis for magnetic particle-based gene delivery, Microfluidics and Nanofluidics, DOI 10.1007/s10404-012-0975-x, 2012.

[3] E. P. Furlani and X. Xue, A model for predicting field directed particle transport in the magnetofection process, Pharm. Res. DOI: 10.1007/s11095-012-0681-0, 2012.

[4] S. A. Khashan, E. P. Furlani, "Coupled particle–fluid transport and magnetic separation in microfluidic systems with passive magnetic functionality", J. Phys. D. Appl. Phys. 46 (12) 125002 doi:10.1088/0022-3727/46/12/125002, 2013.

[5] Biswal, Sibani Lisa, and Alice P. Gast. "Rotational Dynamics of Semiflexible Paramagnetic Particle Chains." [In English]. Phys. Rev. E Stat., Nonlinear, Soft Matter Phys. 69, no. 4-1 (2004): 041406/1-06/9.

[6] Melle, Sonia, and James E. Martin. "Chain Model of a Magnetorheological Suspension in a Rotating Field." [In English]. J. Chem. Phys. 118, no. 21 (2003): 9875-81.